Structure and Stability of the Consecutive Stereoregulated Chiral Phosphorothioate DNA Duplex†

Kenji Kanaori,‡ Yutaka Tamura,‡ Takuya Wada,‡ Masatoshi Nishi,§ Hideyuki Kanehara,|| Takashi Morii,|| Kunihiko Tajima,‡ and Keisuke Makino*,||

Department of Polymer Science and Engineering, Kyoto Institute of Technology, Matsugasaki, Sakyo-ku, Kyoto 606-8585, Japan, Pharmaceutical Sciences, Setsunan University, Nagaotoge-cho, Hirakata 573-0101, Japan, and Institute of Advanced Energy, Kyoto University, Gokasho, Uji 611-0011, Japan

Received April 26, 1999; Revised Manuscript Received October 4, 1999

ABSTRACT: The duplex structures of the stereoregulated phosphorothioate DNAs, [R_p,R_p]- and [S_p,S_p]-[d($GC_{ps}T_{ps}ACG$)] (ps, phosphorothioate; PS-DNA), with their complementary RNA have been investigated by combined use of ^{1}H NMR and restrained molecular dynamics calculation. Compared to those obtained for the unmodified duplex structures (PO-DNA·RNA), the NOE cross-peak intensities are virtually identical for the PS-DNA·RNA hybrid duplexes. The structural analysis on the basis of the NOE restraints reveals that all of the three DNA·RNA duplexes take a A-form conformation and that there is no significant difference in the base stacking for the DNA·RNA hybrid duplexes. On the other hand, the NOE cross-peak intensities of the protons around the central $T_{ps}A$ step of the PS-DNA·DNA duplexes are apparently different from those of PO-DNA·DNA. The chemical shifts of H8/6 and H1′ at the $T_{ps}A$ step are also largely different among PS-DNA·DNAs and PO-DNA·DNA, suggesting that the DNA·DNA structure is readily changed by the introduction of the phosphorothioate groups to the central T_pA step. The structure calculations indicate that all of these DNA·DNA duplexes are B-form although there exist some small differences in helical parameters between the [R_p,R_p]- and [S_p,S_p]PS-DNA·DNA duplexes. The melting temperatures (T_m) were determined for all of the duplexes by plotting the chemical shift change of isolated peaks as a function of temperature. For the PS-DNA·RNA hybrid duplexes, the [S_p,S_p] isomer is less stable than the [R_p,R_p] isomer while this trend is reversed for the PS-DNA·DNA duplexes. Consequently, although the PS-DNA·RNA duplexes take the similar A-form structure, the duplex stability is different between PS-DNA·RNA duplexes. The stability of the DNA·RNA duplexes may not be governed by the A-form structure itself but by some other factors such as the hydration around the phosphorothioate backbone, although the T_m difference of the DNA·DNA duplexes could be explained by the structural factor.

Nucleic acid analogues with modified backbones that have complementary base sequences to their mRNA (antisense) or targeted gene (antigene) have promise as therapeutic agents (*1*). Oligodeoxynucleoside phosphorothioate (PS-oligo),[1] in which one of the nonbridging oxygen atoms in each internucleotide phosphate linkage is replaced by a sulfur atom, has been used extensively as an antisense molecule, and it has been demonstrated in a number of papers that this molecule is potentially antiretroviral (*2*−*4*). In PS-oligo, P-chirality of the internucleotide phosphorothioate linkage (R_p and S_p) generates diastereoisomers, the number of which increases in proportion to 2^{n-1} (n = number of phosphorothioates) (*5*). The variation of the configuration produces different types of PS-oligo diastereoisomers (*6*), for instance, in the duplex stability (*7*−*9*) and recognition by enzymes (*10*, *11*). Comparative NMR studies on structural features of stereospecific PS-oligo duplexes have been carried out for the single P-chirality (R_p and S_p) (*7*, *12*, *13*). It has been reported that there exist only minor effects in the backbone close to the thiophosphate. Since a mixture of PS-oligo isomers (15−20-mer) is employed for therapeutic use, it is important to investigate how the consecutive stereospecific phosphorothioates affect the structure and properties of the PS-oligo duplexes. Recently, duplex structures of [all R_p]-PS-oligos with its complementary RNA strand have been reported (*14*, *15*), and effects of the stereoregulation of the phosphorothioate groups on the duplex structures have been extensively studied.

In the present study, we have focused on the effects of the consecutive stereoregulated phosphorothioate moieties (R_pR_p and S_pS_p) on the structure and stability of the du-

† This work was supported by Grants-in-Aid for Scientific Research (Nos. 11101001 and 08458176) from the Ministry of Education, Science, Sports, and Culture.

* To whom correspondence should be addressed [telephone, +81-(774)-38-3517; fax, +81-(774)-38-3524; e-mail, kmak@iae.kyoto-u.ac.jp].

‡ Kyoto Institute of Technology.

§ Setsunan University.

|| Kyoto University.

[1] Abbreviations: PS-oligo, oligodeoxynucleoside phosphorothioate; CD, circular dichroism; 1D, one dimensional; 2D, two dimensional; DQF-COSY, double-quantum-filtered correlated spectroscopy; TOCSY, total correlation spectroscopy; NOESY, nuclear Overhauser enhancement spectroscopy; E-COSY, exclusive correlation spectroscopy; HMQC, heteronuclear multiple-quantum coherence spectroscopy.

10.1021/bi9909344 CCC: $18.00
Published on Web 11/16/1999

plexes formed by the phosphorothioate DNA and its complementary RNA. The sequence employed for the phosphorothioate DNA is [d($GC_{ps}T_{ps}ACG$)] (ps, phosphorothioate) because we previously reported that this phosphorothioate DNA showed a rather large difference in the melting temperature (T_m) between the [R_p,R_p]- and [S_p,S_p]PS-DNA duplexes (*8*). The T_m difference between these consecutively stereoregulated PS-oligo duplexes was larger than that between singly stereoregulated [R_p]- and [S_p]PS-DNA duplexes (*8*). Since the melting temperature of the duplex of antisense oligodeoxynucleotides with its target strand is considered to be an important factor of antisense effects (*7*, *16*), the relation between the thermal stability and structures of the PS-oligo duplex has been investigated by NMR spectroscopy. In addition to the DNA·RNA duplexes, the phosphorothioate DNA duplexes with its complementary DNA strand have also been studied to compare the effects of the phosphorothioate groups on the duplex structure and stability of DNA·RNA and DNA·DNA duplexes.

MATERIALS AND METHODS

Nomenclature. The numbering system for the r(CGUAGC)·d(GCTACG) and d(CGTAGC)·d(GCTACG) duplexes is

	1	2	3	4	5	6	
5'	C	G	U(T)	A	G	C	
	G	C	Aps	Tps	C	G	5'
	12	11	10	9	8	7	

where ps indicates the phosphorothioate moiety. The unmodified RNA and DNA duplexes [r(CGUAGC)·d(GCTACG) and d(CGTAGC)·d(GCTACG)] were designated as PO-DNA·RNA and PO-DNA·DNA, respectively. The duplexes of the PS-oligo-containing consecutive phosphorothioate stereoisomers [d($GC_{ps}T_{ps}ACG$)] with its complementary RNA strand were designated as [S_p,S_p]PS-DNA·RNA and [R_p,R_p]PS-DNA·RNA, and those with the DNA strand were designated as [S_p,S_p]PS-DNA·DNA and [R_p,R_p]PS-DNA·DNA.

Sample Preparation. The unmodified DNA, RNA, and stereoregulated PS-oligo strands were synthesized on an automatic synthesizer by the phosphoramidite method and purified by gel filtration and reverse-phase HPLC as previously reported (*8*). The concentration of the NMR sample was estimated using the extinction coefficients at 260 nm which were calculated by the nearest neighbor method (*17*). Each duplex was dissolved at a concentration of 4 mM in a buffer containing 10 mM sodium phosphate, 100 mM NaCl, and 0.2 mM ethylenediaminetetraacetic acid (pH 7.0). The solution was heated at 80 °C for 10 min and was gradually cooled to room temperature immediately prior to the NMR measurements.

NMR Spectroscopy. All NMR experiments were carried out on a Bruker ARX-500 spectrometer (500.13 MHz for ^{1}H). A set of 2D NMR spectroscopy experiments [DQF-COSY (*18*), TOCSY (*19*), E-COSY (*20*), NOESY (*21*), ^{1}H−^{31}P HMQC (*22*)] was obtained for all of the duplexes dissolved in the deuterated buffer. NOESY spectra obtained with mixing times of 50, 100, and 200 ms were measured with a 5-s relaxation delay and processed using the programs FELIX 2.3 (Biosym Inc., San Diego, CA) and UXNMR (Bruker). Taking the duplex stability and peak separation into account, temperatures used for the NMR measurements were 15 °C for the RNA duplexes and 10 °C for the DNA duplexes. The jump-and-return NOESY (*23*) was also measured at 5 °C for the sample dissolved in the 90% H_2O/10% D_2O buffer to assign labile protons. ^{1}H and ^{31}P chemical shifts were referred to internal sodium 3-(trimethylsilyl)-propionate-*2,2,3,3-d*$_4$, and external 85% H_3PO_4, respectively. The NMR sample conditions for the T_m measurement were identical to those for the 2D measurements. The 1D spectra were collected after attainment of the equilibration at each temperature. The chemical shift change of well-isolated peaks was plotted as a function of temperature, and the collected data points were fitted to a sigmoidal curve by a nonlinear least squares refinement procedure of ORIGIN (Microcal Software Inc.). All of the T_m values were reproducible from the curves with temperature increasing and decreasing, and the standard deviations were ±0.5−1.0 °C on repetitions of the experiments.

Restrained Molecular Dynamics. The NOESY cross-peak intensities were obtained using a measure-volume tool of FELIX software (Biosym Inc.). The numbers of the interproton distances were 122, 106, and 112 for PO-DNA·RNA, [R_p,R_p]PS-DNA·RNA, and [S_p,S_p]PS-DNA·RNA, respectively, and those were 128, 113, and 125 for PO-DNA·DNA, [R_p,R_p]PS-DNA·DNA, and [S_p,S_p]PS-DNA·DNA, respectively. The initial A- and B-structures were generated using the INSIGHT molecular modeling program (Biosym Inc.), and the unmodified duplexes were used for all of the calculations to avoid the effect of the sulfur atom and its force field parameter. The first approximate structure calculation was conducted on the basis of the NOE restraints derived from 50-ms NOESY spectra. The upper and lower bound corrections of the NOE restraints (a force constant of 20.0 kcal·mol^{-1}·Å^{-2}) were set to be 15% and 10% of the obtained interproton distances, respectively. Restrained molecular dynamics (rMD) and energy minimization (rEM) calculations included 52 backbone torsion angle restraints, 16 hydrogen bond distances between base pairs, and 36 chirality restraints besides the NOE restraints. Since our previous CD results for all of the samples showed that the DNA·RNA duplexes take a kind of A-form and the DNA·DNA duplexes take B-form (*8*), the backbone angle restraints were defined with a force constant of 5.0 kcal·mol^{-1}·rad^{-2} as follows: $245° < \alpha < 355°$, $155° < \beta < 245°$, $5° < \gamma < 90°$, $140° < \epsilon < 300°$, and $150° < \xi < 340°$ (*24*). The simulated rMD calculations of 5 ps at 500 K (Discover module−Amber force field, Biosym Inc.) were carried out to search conformational space for structures consistent with the NMR restraints. The temperature was gradually reduced from 500 to 300 K in the cooling step of 2 ps, and then rMD of 4 ps at 300 K and rEM calculations were carried out. The structures obtained were further refined by the method of iterative relaxation matrix analogue (IRMA, Biosym Inc.) using NOESY spectra with longer mixing times. Atomic rmsd between structures obtained from different starting velocities and identical coordinates were very similar to the values obtained from the different starting coordinates and identical velocities. The 10 resulting structures were averaged and submitted to a final rEM, giving rise to the final average structures. The helical parameters were analyzed using NEWHEL93 (*25*).

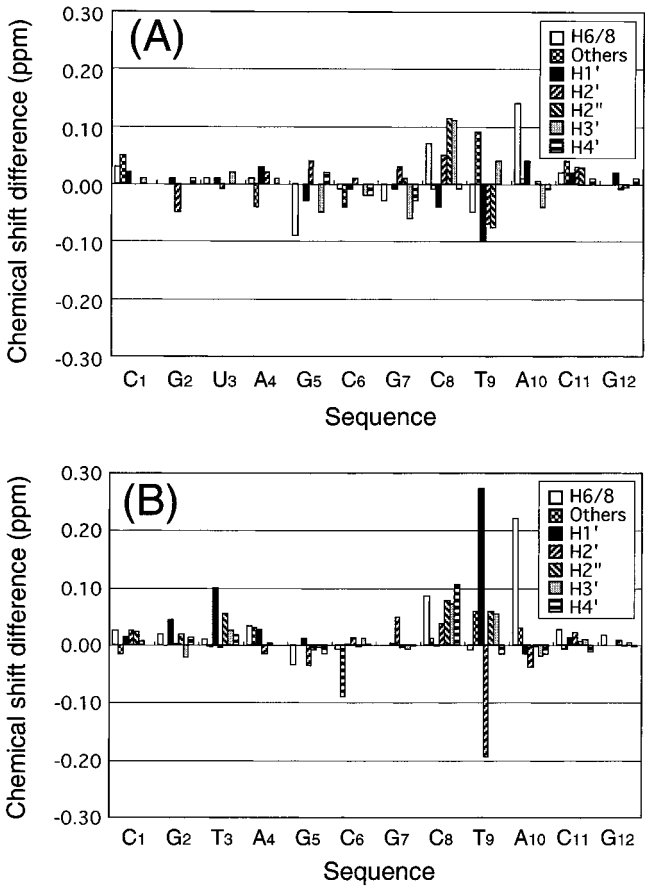

FIGURE 1: ^{1}H chemical shift differences between the stereoregulated phosphorothioate DNA duplexes for all of the nonlabile protons except for H5′/H5″: (A) δ([R_p,R_p]PS-DNA·RNA) − δ([S_p,S_p]PS-DNA·RNA) and (B) δ([R_p,R_p]PS-DNA·DNA) − δ([S_p,S_p]PS-DNA·DNA).

RESULTS

Resonance Assignments. Proton resonances were assigned for all the DNA·RNA and DNA·DNA duplexes from a complete set of homonuclear one- and two-dimensional NMR data using established NMR techniques for nucleic acid analyses (*26*). The assignment of nonexchangeable RNA and DNA protons was achieved by analyzing all regions of the NOESY spectra obtained with various mixing times in combination with TOCSY data, and H5′/5″ proton assignments of T_9 and A_{10} were partly made by ^{1}H−^{31}P HMQC spectra. Two ^{31}P resonances originating from $C_{8ps}T_9$ and $T_{9ps}A_{10}$ were separately observed in the range of 53−57 ppm, which coincides with those reported previously (*16*, *27*). ^{31}P signals from phosphate linkages were severely overlapped in the narrow range around −1 ppm for all of the duplexes. Resonances of the six imino protons for each duplex were also assigned by measuring the samples in H_2O and observing NOE cross-peaks between exchangeable and nonexchangeable protons. The ^{1}H and ^{31}P resonance assignments are summarized in Table S1 (see Supporting Information).

Chemical shift difference ($\Delta\delta$) provides a first approximation of the structure change. The small chemical shift differences observed for the [R_p,R_p]- and [S_p,S_p]PS-DNA·RNA duplexes ($|\Delta\delta| < 0.15$ ppm) (Figure 1A) coincide with the previous result of the phosphorothioate DNA·RNA duplexes (*12*, *13*) where the maximum $|\Delta\delta|$ was reported to be 0.05 ppm. The small chemical shift differences observed for the DNA·RNA duplexes indicate that little structure variation occurs to the DNA·RNA duplexes. On the other hand, the chemical shift differences between the two isomeric PS-DNA·DNA duplexes were found to be larger than those between the PS-DNA·RNA hybrid duplexes. The differences in chemical shift between [R_p,R_p]- and [S_p,S_p]PS-DNA·DNA are shown in Figure 1B, where the T_9-H1′, T_9-H2′, and A_{10}-H8 protons show large differences ($|\Delta\delta| > 0.2$ ppm) between the PS-DNA·DNA duplexes. However, the T_9-H6 proton located between the phosphorothioate groups exhibits only a small difference ($|\Delta\delta| = 0.01$ ppm) between the PS-DNA·DNAs. These results indicate that the influence of the phosphorothioate moiety at the $C_{8ps}T_9$ step on the chemical shift difference likely differs from that at the $T_{9ps}A_{10}$ step. The result of the chemical shift changes suggests that the structure change caused by the phosphorothioate group is sequence-dependent for the PS-DNA·DNA duplexes. Since single-stranded [R_p,R_p]- and [S_p,S_p]-d($GC_{ps}T_{ps}ACG$) showed very similar chemical shifts for H8/H6 protons (<0.02 ppm) (data not shown), the chemical shift change of the A_{10}-H8 proton may reflect the structural differences between the two isomeric PS-DNA·DNA duplexes.

To examine the effect of the phosphorothioate group on the chemical shifts, the chemical shift differences were also obtained between the modified and unmodified duplexes (Figures S1 and S2; see Supporting Information). For the DNA·RNA hybrid duplexes (Figure S1), the chemical shift difference pattern between the modified and unmodified duplexes was almost identical for [R_p,R_p]- and [S_p,S_p]PS-DNA·RNA: The H2′/H2″/H3′ protons of C_8 and the H3′ proton of T_9 of both of the PS-DNA·RNA duplexes showed large downfield shifts from PO-DNA·RNA. The downfield shifts of these protons for [R_p,R_p]PS-DNA·RNA were slightly larger than those for [S_p,S_p]PS-DNA·RNA. Since these chemical shift differences were observed only around the protons near phosphorothioate groups, the differences may be attributed to the direct effect of the phosphorothioate groups but not to the structural change (*15*). For the DNA·DNA duplexes (Figure S2), the C_8- and T_9-H3′ protons of the stereospecific PS-DNA·DNAs were also shifted downfield, as compared to those of the PO-DNA·DNA duplex. Outstanding shifts were observed for A_{10}-H8 of [R_p,R_p]PS-DNA·DNA and T_9-H1′ of [S_p,S_p]PS-DNA·DNA. Since there was little difference in the chemical shifts of the H3′ protons between [R_p,R_p]- and [S_p,S_p]PS-DNA·DNA, the observed downfield shifts of the H3′ protons of PS-DNA·DNAs from PO-DNA·DNA may be attributed to the change in the shielding effect by the substitution of the phosphorothioate group for the phosphate group (*15*). However, the above-mentioned large shifts such as T_9-H1′ and A_{10}-H8 may be due to the structural change from the wild-type duplex.

Analysis of NOESY and E-COSY Spectra. To investigate the duplex conformations in detail, NOESY and E-COSY spectra were measured for all the duplexes. To take advantage of the better spectral resolution in F_2, the cross-peaks above the diagonal of the well-digitized E-COSY spectra were used to measure the coupling constants. The obtained J coupling data ($^3J_{1'2'}$, $^3J_{1'2''}$) are also listed in Table S1. Figure 2 shows 50-ms NOESY spectra of the DNA·RNA duplexes, PO-DNA·RNA, [S_p,S_p]PS-DNA·RNA, and [R_p,R_p]PS-DNA·RNA. The comparison of the NOESY spectra of the DNA·RNA duplexes did not show prominent

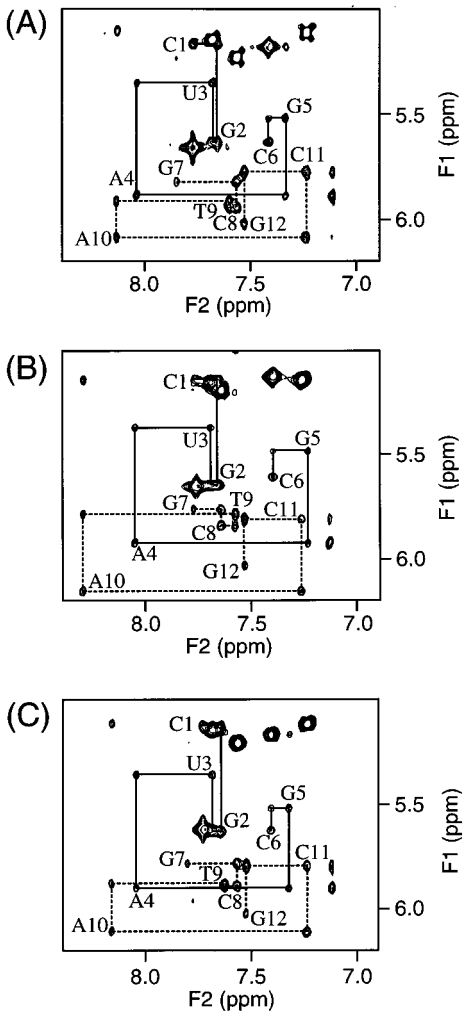

FIGURE 2: ^{1}H 2D NOESY spectra (mixing time 50 ms) collected at 15 °C for (A) PO-DNA·RNA, (B) [S_p,S_p]PS-DNA·RNA, and (C) [R_p,R_p]PS-DNA·RNA in the aromatic to H1′ region. Sequential NOE connectivities for a strand of r(CGUAGC) are indicated by a solid line, and those for d(GCTACG) are indicated by a broken line. Intraresidue NOE connectivities between H1′ and H8/H6 are indicated by residue names.

differences in the NOE cross-peak intensities. The distance restraints derived from the NOESY spectrum were almost identical for the three DNA·RNA duplexes, and the comparison of the distance restraints between the DNA·RNA duplexes showed that the distance differences for the same proton pairs were less than 0.5 Å. This indicates that all of the DNA·RNA duplexes take a quite similar conformation.

The conformation of the DNA·RNA duplexes was found to be an overall A-form conformation by the following observations: (i) The H8/H6(i)−H2′(i−1) NOESY cross-peaks of the RNA strand at 50 ms were much stronger than any of the DNA H8/H6(i)−H2′/H2″(i, i−1) cross-peaks (data not shown). (ii) The H1′−H2′ coupling constants of the riboses were not detectable in the DQF-COSY spectra of all of the DNA·RNA duplexes. (iii) The H8 protons of the purine residues moved upfield by 0.3−0.5 ppm while the H6 protons of the pyrimidine residues moved downfield by ∼0.2 ppm compared to the corresponding DNA·DNA duplex. All the H1′s of the DNA·RNA duplexes moved upfield by 0.3−0.8 ppm from those of DNA·DNA duplexes. These chemical shift observations also indicate that the conformations for the hybrid DNA·RNA duplexes are similar to the A-form conformation (*28*, *29*). The previous detailed report about the DNA·RNA duplexes containing a single stereoregulated phosphorothioate moiety demonstrated that the deoxyriboses underwent pucker transitions between the S- and N-type, while the puckering of the ribose was the N-type (*12*, *13*). Our qualitative analysis of the NOESY and E-COSY spectra also indicates that all of the RNA residues have N-type and C3′-endo and the DNA residues have O4′-endo or C2′-endo. In addition, we measured ^{1}H−^{31}P HMQC spectra for the PS-DNA·RNAs to obtain information about phosphorothioate backbone conformation. Besides cross-peaks between P and H3′/H5′/H5″ arising from $^3J_{PH'}$, a rather strong P−H4′ cross-peak from $^4J_{PH4'}$ was observed for $T_{9ps}A_{10}$ but not for $C_{8ps}T_9$ for both of the PS-DNA·RNAs. This result indicates that the backbone dihedral angles (γ, β) are different between the two phosphorothioate groups and that the atoms in the sequence P−O5′−C5′−C4′−H4′ at the $T_{9ps}A_{10}$ of the PS-DNA·RNA duplexes are well arranged in a planar W-shaped conformation where γ and β adopt a gauche(+) and a trans conformation, respectively (*22*, *30*).

For the DNA·DNA duplexes, the situation is different from the DNA·RNA duplexes. Figure 3 shows the expanded H8/H6−H1′ regions of the 50-ms NOESY spectra for the three DNA duplexes: PO-DNA·DNA, [S_p,S_p]PS-DNA·DNA, and [R_p,R_p]PS-DNA·DNA. An overall right-handed B-form structure was ascertained for all of the DNA duplexes from the observation of H8/H6(i)−H5/CH$_3$(i+1) NOEs and of the NOE intensity pattern involving the H2′/2″ and H8/H6 protons: H2′(i)−H8/H6(i) ≫ H2″(i−1)−H8/H6(i) > H2′-(i−1)−H8/H6(i) (*31*). The sugar pucker and glycosidic bond conformations probably lie in the O1′-endo to C2′-endo and anti ranges, respectively, on account of intranucleotide sugar−base NOE patterns [H2′(i)−H8/H6(i) ≫ H1′(i)−H8/H6(i) > H3′(i)−H8/H6(i)] and coupling constant data from E-COSY spectra. The coupling constant values exhibited that sugar puckering modes for PO-DNA·DNA and PS-DNA·DNAs were almost identical. ^{1}H−^{31}P HMQC spectra of PS-DNA·DNAs showed the same tendency as those of PS-DNA·RNAs: a strong H4′−P cross-peak for $T_{9ps}A_{10}$ and a weak one for $C_{8ps}T_9$. This indicates that PS-DNA·DNAs also adopt the backbone torsion angles of γ^+ and β^t at $T_{9ps}A_{10}$, as well as PS-DNA·RNAs.

The difference in NOE cross-peak intensities between PO-DNA·DNA and PS-DNA·DNAs was observed for NOEs from the aromatic to H1′ region. It has been previously reported that, in B-form DNA, the distance from H8/H6(i) to H1′(i) should be invariant from residue to residue (3.6−3.9 Å) over the range of glycosidic torsion angles (χ = −120° to −180°) and that the distance from the (i)-aromatic proton to the sugar H1′ proton of the previous residue is typically shorter than that to its own sugar H1′ proton. Therefore, the cross-peak to the previous H1′ is usually stronger than to its own H1′. This pattern exists for all of the residues in PO-DNA·DNA (Figure 3A). For example, the A_{10}-H8 to A_{10}-H1′ cross-peak was almost equal to the A_{10}-H8 to T_9-H1′ cross-peak for PO-DNA·DNA. However, the anomaly can be seen in the sequential NOEs in the $T_{3p}A_4$ and $T_{9ps}A_{10}$ steps for PS-DNA·DNAs (Figure 3B,C). The interresidue NOEs were much weaker than the intraresidue ones: The A_{10}-H8 to T_9-H1′ cross-peak of the PS-DNA·DNAs was excessively weaker than the other (i) to (i−1)

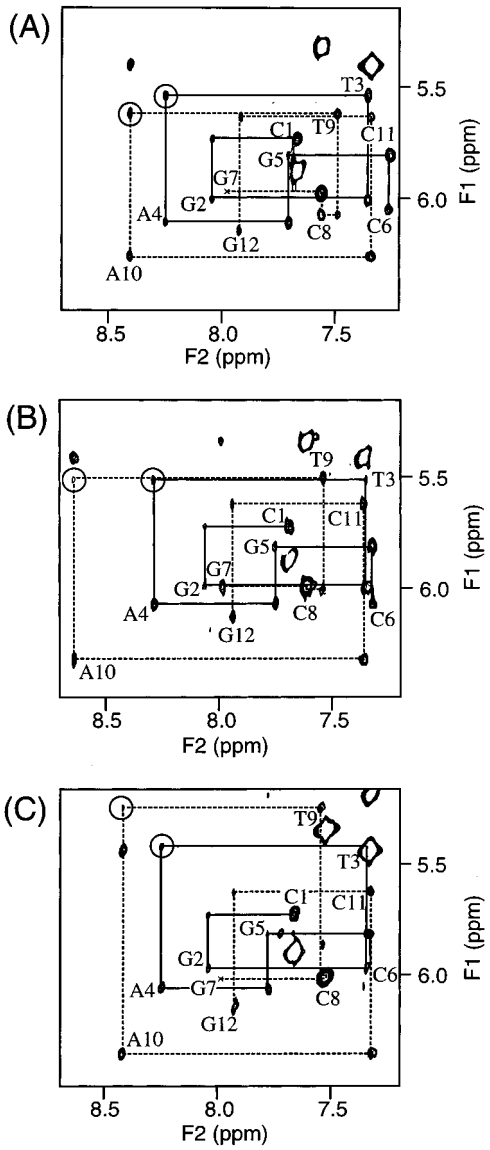

FIGURE 3: ^{1}H 2D NOESY spectra (mixing time 50 ms) collected at 10 °C for (A) PO-DNA·DNA, (B) [S_p,S_p]PS-DNA·DNA, and (C) [R_p,R_p]PS-DNA·DNA in the aromatic to H1′ region. Sequential connectivities for a strand of d(CGTAGC) are indicated by a solid line, and those for d(GCTACG) are indicated by a broken line. Intraresidue NOEs between H1′ and H8/H6 are indicated by the residue names. Cross-peaks indicated by a circle are weak sequential NOE cross-peaks around the phosphorothioate groups.

cross-peaks. These significant variations in the cross-peak intensities reflect that the distances can vary by ~0.7 Å. Concomitantly, sequential NOE connectivities between H2″ and H8/H6 resonances appeared weak at the $T_{9ps}A_{10}$ step. Such weak sequential NOE cross-peaks were reported for the T_pA step of [d(CGAGGTTTAAACCTCG)]$_2$ (*32*). These changes of NOE cross-peak intensities were particularly evident in the case of [R_p,R_p]PS-DNA·DNA.

Structure Calculation. The investigation on the helical parameters provides us with information about the local conformation of the duplexes in detail. The molecular dynamics calculations were performed with the distance restraints derived from well-resolved NOE cross-peak intensities. For all of the duplexes, the pairwise root-mean-square deviations (rmsd) calculated for 10 structures from each run were below 0.4 Å for the two most divergent structures, indicating that good convergence has been reached. Energy terms of the final averaged structure, a largest restraint violation, and the number of the violation (>0.2 Å) were also obtained for each duplex and are collected in Table S2 (see Supporting Information). To make a further assessment of the final averaged structures, an average restraint deviation, Δd_{av} (*24*), was calculated for each duplex. The average distance deviation is $\Delta d_{av} = (1/N)\sum\Delta r$, where the summation is taken over all restrained distances including the terminal base pairs, N is the number of restraints, and Δr is the violation from the distance restraints. For the DNA·RNA duplexes, the values of Δd_{av} were 0.03 Å, while for the DNA·DNA duplexes, those were 0.04−0.05 Å. In addition, no dihedral violation was observed. These results indicate that all the distances were consistent with the final structures.

The structures of the DNA·RNA duplexes obtained were in the conformational range expected for A-form, as shown by the smaller rmsd between the final structure and the A-form starting structure of 3.0−3.2 Å compared to 3.8−4.0 Å between those structures and the B-form starting structure (Table S2). For the DNA·DNA duplexes, the rmsd values between the final averaged structure and the starting structure were 3.5−3.6 Å for the A-form starting structure and 3.2−3.3 Å for the B-form starting structure (Table S2). It indicates that the final structures of the DNA·DNA duplexes are in the conformational range between A- and B-form structures.

The rmsd values between final averaged structures of [R_p,R_p]PS-DNA·RNA, [S_p,S_p]PS-DNA·RNA, and PO-DNA·RNA were 0.6−0.7 Å, and these structures are overlaid in Figure 4A. The structural differences between three DNA·RNA duplexes were small. On the other hand, rmsd values between the final averaged structures of [R_p,R_p]PS-DNA·DNA, [S_p,S_p]PS-DNA·DNA, and PO-DNA·DNA were around 0.7−1.0 Å. The final structures of PS-DNA·DNAs were rather different from that of PO-DNA·DNA with respect to the deoxyribose positions, which could be attributed to the weak NOE cross-peaks in the $T_{ps}A$ step (Figure 4B).

Selected helical parameters (roll, twist, rise, and propeller twist) are given in Table 1. The roll reached a maximum positive value for all of the duplexes at the T_pA or $T_{ps}A$ step. The large positive roll value at the T_pA step was reported for other duplex structures which have a T_pA step (*32*). The averaged twist values for the DNA·RNA duplexes were smaller than those for the DNA·DNA duplexes, supporting the fact that the hybrid DNA·RNA duplexes take A-form while the DNA·DNA duplexes take B-form. The helical twist varied within the three DNA·DNA duplexes at the positions around the phosphorothioate groups. For the DNA·RNA duplexes, the rise parameters of [S_p,S_p]PS-DNA·RNA were different from those of the other DNA·RNA duplexes, while those for the DNA·DNA duplexes were constant. The propeller twist ranged from −20° to −10°, which is almost identical for all the duplexes. A complete list is given as Supporting Information. However, no specific helical parameters could be defined for interpreting the structural differences among PS-DNA·DNAs and PO-DNA·DNA because most of the other conformational parameters calculated by NEWHEL93 are interrelated as shown previously (*33*, *34*).

Melting Temperatures of the Duplexes. To examine whether the stability of the duplexes could correlate with

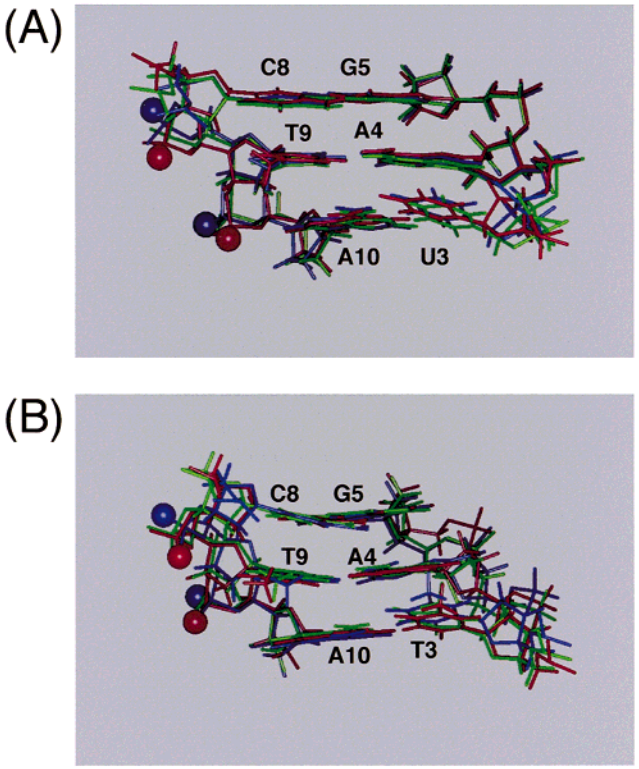

FIGURE 4: (A) Base pairing of G_5·C_8 (top), A_4·T_9 (middle), and U_3·A_{10} (bottom) looking perpendicular to the major helix axis in [R_p,R_p]PS-DNA·RNA (red), [S_p,S_p]PS-DNA·RNA (blue), and PO-DNA·RNA (green). Half size of van der Waals surfaces is shown for sulfur atoms of the duplexes. (B) Base pairing of G_5·C_8 (top), A_4·T_9 (middle), and T_3·A_{10} (bottom) looking perpendicular to the major helix axis in [R_p,R_p]PS-DNA·DNA (red), [S_p,S_p]PS-DNA·DNA (blue), and PO-DNA·DNA (green).

the structural differences, the thermal melting profile was investigated for all of the duplexes by ^{1}H NMR spectra. The duplex stability is also considered to be important for the estimation of antisense effects of modified DNA. On the basis of the temperature dependence of chemical shift change of isolated nonexchangeable proton signals, the T_m values were determined, and these isolated protons were cooperatively shifted with the temperature change. The T_m values for PO-DNA·RNA, [S_p,S_p]PS-DNA·RNA, and [R_p,R_p]PS-DNA·RNA were 43, 38, and 42 °C, respectively (Figure 5A). The [S_p,S_p]PS-DNA·RNA duplex was less stable than the [R_p,R_p]PS-DNA·RNA and PO-DNA·RNA duplexes. On the other hand, the T_m values for the DNA·DNA duplexes were 44, 42, and 40 °C for PO-DNA·DNA, [S_p,S_p]PS-DNA·DNA, and [R_p,R_p]PS-DNA·DNA, respectively (Figure 5B). These results demonstrate that the introduction of the stereoregulated phosphorothioate groups causes considerably large change in the stability of the PS-DNA·RNA duplexes and rather small change in the T_m values between the PS-DNA·DNA duplexes, both of which are less stable than PO-DNA·DNA. We also observed the temperature dependence of imino proton signals to obtain information about the duplex stability. The imino protons at the terminal and penultimate base pairs disappeared around 15−20 and 25−30 °C, respectively, and all the imino proton signals disappeared below 35 °C, much lower than the T_m values determined by the chemical shift change. Since the line broadening of the imino protons would depend on the fluctuation of the base pairs or the fast exchange between the imino proton and water, we employed the T_m values obtained by the chemical shift change in the present paper.

DISCUSSION

The structure of the PS-oligo·RNA hybrid duplex which is considered to be a therapeutically active form has been studied intensively (*12*−*14*). In this study, as shown in Figure 4A, we have determined that there exists no significant structural difference among [R_p,R_p]PS-DNA·RNA, [S_p,S_p]PS-DNA·RNA, and PO-DNA·RNA. This structural resemblance of the DNA·RNA duplexes coincides with the previously reported results on the phosphorothioate DNA·RNA duplexes containing a single phosphorothioate (*12*, *13*). Analogously, it was recently reported that [all R_p]PS-oligo duplexes with its complementary RNA take an A-form structure similar to a corresponding natural-type DNA·RNA duplex (*14*, *15*). This structural coincidence is explained as follows: All of these DNA·RNA duplexes take an A-form conformation. Since an A-form structure opens toward the minor groove (typical roll angle = 10°) (*35*, *36*), the steric hindrance around the phosphorothioate moieties of the PS-oligo·RNA hybrid duplexes would be weakened by taking the A-form conformation. For instance, it was reported that a phosphorodithioate-modified oligonucleotide decamer duplex, d(CGCTT$_{ps2}$AAGCG)$_2$ (ps2, phosphorodithioate), would take an A-form structure at the T$_{ps2}$A step (*37*). Thus, the substitution of the nonbridging oxygen atom in the phosphate backbone with the sulfur atom may be in favor of the A-form-like structure. Our preliminary circular dichroism (CD) study on [all R_p]- and [all S_p]PS-DNA·RNA duplexes of the same sequence has revealed little difference in the CD spectral pattern even between both of the completely stereoregulated PS-DNA·RNA duplexes, which will be published elsewhere. Since a hybrid DNA·RNA duplex itself is inclined to take an overall A-form conformation, the introduction of the consecutive phosphorothioate groups may hardly alter the structure of the PS-oligo duplex with its complementary RNA strand. This structural similarity between the modified and unmodified DNA·RNA duplexes of the same sequence may explain why phosphorothioate DNA·RNA complexes can be recognized and digested by RNase H and substantiate therapeutic uses of the stereoisomeric PS-oligo mixture.

On the other hand, it is shown that the introduction of the phosphorothioate group to the DNA·DNA duplex causes structure change at the T$_{ps}$A step. In particular, the weak sequential NOE cross-peaks of [R_p,R_p]PS-DNA·DNA at the central T$_{ps}$A step indicate the distorted structure which differs from a typical B-DNA. This structural distortion of the phosphorothioate DNA·DNA duplex may be caused by the steric hindrance between the phosphorothioate group and the deoxyribose moiety since the distance between the R_p sulfur atom and the deoxyribose protons is smaller for B-form DNA than for A-form DNA (Figure 4). The distorted T$_{ps}$A base step of the PS-DNA·DNAs is also supported by the large chemical shift deviations of T_9-H1′ and A_{10}-H8 from those of the PO-DNA·DNA, respectively. Since protons such as H1′ and H8 are apart from the phosphorothioate moiety, the direct electrostatic effect of the phosphorothioate moieties on their chemical shifts should be very small. Thus, the observed large differences in the chemical shift are likely caused by differences in the structure between the DNA·DNA duplexes. It is known that the base stacking of the

Table 1: Selected Conformational Parameters of the Duplexes:[a] (a) Roll, (b) Twist, (c) Rise, and (d) Propeller Twist

(a) Roll (deg)

		PS-DNA·RNA				PS-DNA·DNA	
base step	PO-DNA·RNA	[R_p,R_p]	[S_p,S_p]	base step	PO-DNA·DNA	[R_p,R_p]	[S_p,S_p]
G_2-U_3	3	3	−1	G_2-T_3	3	3	2
U_3-A_4	19	20	20	T_3-A_4	15	15	14
A_4-G_5	2	2	1	A_4-G_5	2	−2	3

(b) Twist (deg)

		PS-DNA·RNA				PS-DNA·DNA	
base step	PO-DNA·RNA	[R_p,R_p]	[S_p,S_p]	base step	PO-DNA·DNA	[R_p,R_p]	[S_p,S_p]
G_2-U_3	36	37	32	G_2-T_3	35	31	30
U_3-A_4	33	38	34	T_3-A_4	37	33	42
A_4-G_5	33	28	29	A_4-G_5	33	41	36

(c) Rise (Å)

		PS-DNA·RNA				PS-DNA·DNA	
base step	PO-DNA·RNA	[R_p,R_p]	[S_p,S_p]	base step	PO-DNA·DNA	[R_p,R_p]	[S_p,S_p]
G_2-U_3	1.7	1.9	2.4	G_2-T_3	2.7	3.0	2.8
U_3-A_4	2.9	2.8	3.5	T_3-A_4	3.0	3.1	3.2
A_4-G_5	2.6	2.4	2.8	A_4-G_5	2.8	3.1	3.0

(d) Propeller Twist (deg)

		PS-DNA·RNA				PS-DNA·DNA	
bae pair	PO-DNA·RNA	[R_p,R_p]	[S_p,S_p]	base pair	PO-DNA·DNA	[R_p,R_p]	[S_p,S_p]
G_2	−15	−14	−14	G_2	−15	−15	−8
U_3	−17	−19	−16	T_3	−16	−19	−18
A_4	−13	−14	−16	A_4	−15	−10	−18
G_5	−6	−15	−9	G_5	−16	−14	−18

[a] The parameters were obtained for the final energy-minimized structure after 10 structures were averaged.

T_pA step is theoretically the most unstable of all possible base-step combinations (*38*) and is easily deformed by binding to another molecule such as a drug or protein (*39*−*42*). Thus the local structure of the flexible part such as the T_pA step in the B-form duplex would be easily affected by the introduction of the phosphorothioate group. From a structural point of view, it is of interest whether this characteristic feature of the central $T_{ps}A$ step is retained in other longer sequences. The crystalline structure of a self-complementary phosphorothioate DNA duplex, [R_p]-d($G_{p-s}C_pG_{ps}C_pG_{ps}C)_2$, was reported to show a B-form duplex and to consist of two different backbone conformations (*43*). This backbone flexibility observed for the [R_p]PS-oligo DNA·DNA duplex may be related to the structural distortion observed for the $T_{ps}A$ step, which is probably less stable than a $G_{ps}C$ step. The flexibility of the central T_pA step was also reported to be retained in different sequences (*44*). These results suggest that the structural feature at the central $T_{ps}A$ step might be observed for longer PS-oligo DNA·DNA duplexes.

It is also shown in the present study that T_m values of the PS-oligo duplexes vary depending on the chirality of the phosphorothioate and on the nature of the complementary strand (DNA·RNA or DNA·DNA). The T_m value of [S_p,S_p]-PS-DNA·RNA is significantly lower than those of [R_p,R_p]-PS-DNA·RNA and PO-DNA·RNA. Since the three hybrid DNA·RNA duplexes take a similar conformation, the destability of [S_p,S_p]PS-DNA·RNA could not be clarified from a view of the DNA·RNA conformations. As previously reported, the duplex stability greatly depends on the hydration of the water molecules, and the water molecules are located along the major and minor grooves (*45*). Since the three DNA·RNA duplexes in this study take the similar A-form conformation, the destability of [S_p,S_p]PS-DNA·RNA may be attributed to the change in the water network around the phosphorothioate groups. The sulfur atoms of [S_p,S_p]PS-DNA·RNA are directed to the minor groove, which is shallow for the A-form conformation. The water network in the shallow minor groove might easily be altered by the introduction of the [S_p]-phosphorothioate linkage, while the water structure in the deep major groove is possibly unaffected by the [R_p]-phosphorothioate linkages. On the other hand, in the case of the DNA·DNA duplex, [R_p,R_p]-PS-DNA·DNA is less stable than [S_p,S_p]PS-DNA·DNA. It is noteworthy that [R_p,R_p]PS-DNA·DNA whose T_m value is lower than that of PO-DNA·DNA shows much weaker sequential NOEs at the central $T_{ps}A$ step. Our previous study also showed that the T_m values of PS-oligo DNA·DNA duplexes containing a single phosphorothioate group differ largely between R_p and S_p when the phosphorothioate group is introduced to the T_pA step (*8*). Hence, the $T_{ps}A$ step of the PS-DNA·DNA duplexes may be flexible and allow conformational variation under the influence of the phosphorothioate group. Consequently, the stability of PS-DNA·RNA hybrids is mainly dominated by the water hydration while that of PS-DNA·DNA duplexes is likely dominated by the structural difference.

It is important to examine whether the modification and stereoregulation of the phosphate backbone could affect the therapeutic effect. The DNA·RNA hybrid duplex containing the PS-oligo of [all R_p] configurations was found to be more susceptible to the degradation by RNase H, as compared to the [all S_p]PS-oligo, and the DNA·RNA duplex containing R_p linkages was more stable than that containing S_p linkages (*11*), which is also shown in this study. These studies suggest that the therapeutic effects of PS-oligos are changed by the

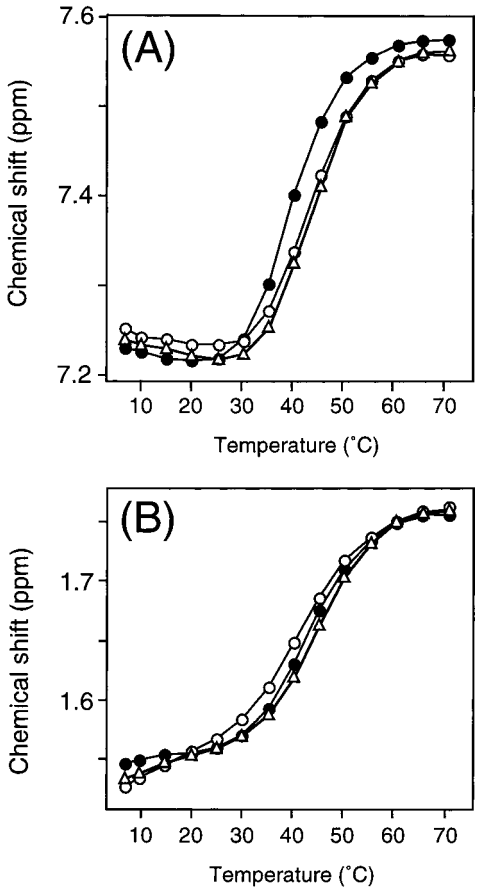

FIGURE 5: Chemical shift change as a function of temperature of (A) C_{11} H6 of the three DNA·RNA duplexes and of (B) the T_9 CH_3 proton of the DNA·DNA duplexes. Open triangles indicate PO-DNA·RNA and PO-DNA·DNA, open circles indicate [R_p,R_p]-PS-DNA·RNA and [R_p,R_p]PS-DNA·DNA, and closed circles indicate [S_p,S_p]PS-DNA·RNA and [S_p,S_p]PS-DNA·DNA.

stereoregulation of the phosphorothioate backbone and that PS-oligos with the [all R_p] configurations are favorable to the therapeutic use. The small structural difference between the PS-DNA·RNA hybrid duplexes with the consecutive phosphorothioate groups in this study reinforces the advantage of the PS-oligo with the R_p linkages whose T_m is higher than that with the S_p linkages. An interest in the relationship between structure and stereoregulation of DNA backbone is increasing, and an antisense DNA·RNA hybrid containing alternating chirally pure [R_p]-methylphosphonates was also recently studied by NMR (*46*). The stereocontrolled chemical synthesis of PS-oligo has been demonstrated (*11*, *47*−*50*), leading to the evaluation of the relation between structure and true antisense effect of PS-oligo. In this study, we have shown that the structure of the DNA·RNA duplex is not influenced by the introduction of the stereoregulated phosphorothioate group, while the duplex stability is affected. In the case of the molecular design of short PS-oligos as an antisense, the stereoregulation of the phosphorothioate group in the R_p configuration may be effective for increasing the melting temperature without structural change. In addition, the structural variation observed for the DNA·DNA duplexes suggests that there are some possibilities of the structural change by the stereoregulation of the phosphorothioate group in the case of other DNA structures such as DNA triplex, G-quartet, and i-motif which are other important applications of PS-oligos. Since the hexamer sequences studied here are very short, the influence of base-pair fraying at the terminal and penultimate base pairs may not be ruled out. The stereocontrolled synthesis of longer PS-oligos will aid in verifying the present results.

ACKNOWLEDGMENT

We thank Ms. Sae Ishikawa for her assistance with measuring NMR spectra.

SUPPORTING INFORMATION AVAILABLE

^{1}H assignment of all of the six duplexes and ^{31}P assignment of the phosphorothioate groups (Table S1), chemical shift differences between the unmodified and modified duplexes for the DNA·RNA and DNA·DNA duplexes (Figures S1 and S2), respectively, final energy parameters and structure calculation results of all of the duplexes (Table S2), and helical parameters of the DNA·RNA and DNA·DNA duplexes (Figures S3 and S4), respectively. This material is available free of charge via the Internet at http://pubs.acs.org.

REFERENCES

1. Crooke, S. T. (1995) *Therapeutic applications of oligonucleotides*, R. G. Landes Co., Austin, TX.
2. Agrawal, S., Goodchild, J., Civeira, M. P., Thornton, A. H., Sarin, P. S., and Zamecnik, P. C. (1988) *Proc. Natl. Acad. Sci. U.S.A. 85*, 7079−7083.
3. Majumdar, C., Stein, C. A., Cohen, J. S., Broder, S., and Wilson, S. H. (1989) *Biochemistry 28*, 1340−1346.
4. Stein, C. A., and Cheng, Y. C. (1993) *Science 261*, 1004−1012.
5. Stec, W. J., Zon, G., and Egan, W. (1984) *J. Am. Chem. Soc. 106*, 6077−6079.
6. Stec, W. J., and Wilk, A. (1994) *Angew. Chem. 106*, 747−761.
7. LaPlanche, L. A., James, T. L., Powell, C., Wilson, W. D., Uznanski, B., Stec, W. J., Summers, M. F., and Zon, G. (1986) *Nucleic Acids Res. 14*, 9081−9093.
8. Kanehara, H., Wada, T., Mizuguchi, M., and Makino, K. (1996) *Nucleosides Nucleotides 15*, 1169−1178.
9. Stec, W. J., Grajkowski, A., Kobylanska, A., Karwowski, B., Koziolkiewicz, M., Misiura, K., Okruszek, A., Wilk, A., Guga, P., and Boczkowska, M. (1995) *J. Am. Chem. Soc. 117*, 12019−12029.
10. Kurpiewski, M. R., Koziolkiewicz, M., Wilk, A., Stec, W. J., and Jen-Jacobson, L. (1996) *Biochemistry 35*, 8846−8854.
11. Koziolkiewicz, M., Krakowiak, A., Kwinkowski, M., Boczkowska, M., and Stec, W. J. (1995) *Nucleic Acids Res. 23*, 5000−5005.
12. González, C., Stec, W., Kobylanska, A., Hogrefe, R. I., Reynolds, M., and James, T. L. (1994) *Biochemistry 33*, 11062−11071.
13. González, C., Stec, W., Reynolds, M. A., and James, T. L. (1995) *Biochemistry 34*, 4969−4982.
14. Bachelin, M., Hessler, G., Kurz, G., Hacia, J. G., Dervan, P. B., and Kessler, H. (1998) *Nat. Struct. Biol. 5*, 271−276.
15. Furrer, P., Billeci, T. M., Donati, A., Kojima, C., Karwowski, B., Sierzchala, A., Stec, W. J., and James, T. L. (1999) *J. Mol. Biol. 285*, 1609−1622.
16. Jaroszewski, J. W., Clausen, V., Cohen, J. S., and Dahl, O. (1996) *Nucleic Acids Res. 24*, 829−834.
17. Fasman, D. G., Ed. (1975) *Handbook of Biochemistry and Molecular Biology*, 3rd ed., Vol. 1, p 589, CRC Press, Cleveland, OH.
18. Piantini, U., Sørensen, O. W., and Ernst, R. R. (1982) *J. Am. Chem. Soc. 104*, 6800−6801.
19. Davis, D. G., and Bax, A. (1985) *J. Am. Chem. Soc. 107*, 2820−2821.

20. Bax, A., and Lerner, L. (1988) *J. Magn. Reson. 79*, 429−438.
21. Jeener, J., Meier, B. H., Bachmann, P., and Ernst, R. R. (1979) *J. Chem. Phys. 71*, 4546−4553.
22. Blommers, M. J. J., van de Ven, F. J. M., van der Marel, G. A., van Boom, J. H., and Hilbers, C. W. (1991) *Eur. J. Biochem. 201*, 33−51.
23. Williamson, J. R., and Boxer, S. G. (1989) *Biochemistry 28*, 2819−2831.
24. Mujeeb, A., Kerwin, S. M., Kenyon, G. L., and James, T. L. (1993) *Biochemistry 32*, 13419−13431.
25. Dickerson, R. E., Bansal, M., Calladine, C. R., Diekmann, S., Hunter, W. N., Kennard, O., Lavery, R., Nelson, H. C. M., Saenger, W., Shakked, Z., Sklenar, H., Soumpasis, D. M., Tung, C.-S., Wang, A. H.-J., and Zhurkin, V. B. (1989) *EMBO J. 8*, 1−4.
26. Wüthrich, K. (1986) *NMR of Proteins and Nucleic Acids*, Wiley-Interscience, New York.
27. Eckstein, F., and Jovin, T. M. (1983) *Biochemistry 22*, 4546−4550.
28. Chou, S.-H., Flynn, P., and Reid, B. (1989) *Biochemistry 28*, 2430−2434.
29. Chou, S.-H., Flynn, P., and Reid, B. (1989) *Biochemistry 28*, 2435−2443.
30. Blommers, M. J. J., Tondelli, L., and Garbesi, A. (1994) *Biochemistry 33*, 7886−7896.
31. Clore, G. M., and Gronenborn, A. M. (1985) *FEBS Lett. 179*, 187−198.
32. Lingbeck, J., Kubinec, M. G., Miller, J., Reid, B. R., Drobny, G. P., and Kennedy, M. A. (1996) *Biochemistry 35*, 719−734.
33. Yanagi, K., Privé, G. G., and Dickerson, R. E. (1991) *J. Mol. Biol. 217*, 201−214.
34. Tereshko, V., Urpi, L., Malinina, L., Huynh-Dinh, T., and Subirana, J. A. (1996) *Biochemistry 35*, 11589−11595.
35. Arnott, S., and Hukins, D. W. L. (1972) *Biochem. Biophys. Res. Commun. 47*, 1504−1510.
36. Arnott, S., and Hukins, D. W. L. (1973) *J. Mol. Biol. 81*, 93−105.
37. Cho, Y., Zhu, F. C., Luxon, B. A., and Gorenstein, D. G. (1993) *J. Biomol. Struct. Dyn. 11*, 685−702.
38. Rein, R., Ornstein, R. L., and Macelroy, R. D. (1978) *Proc. Indian Acad. Sci., Sect. B 87B*, 135−145.
39. Shakked, Z., Guzikevich-Guerstein, G., Frolow, F., Rabinovich, D., Joachimiak, A., and Sigler, P. B. (1994) *Nature 368*, 469−473.
40. Goodsell, D. S., Kaczor-Grzeskowiak, M., and Dickerson, R. E. (1994) *J. Mol. Biol. 239*, 79−96.
41. Urpí, L., Tereshko, V., Malinina, L., Huynh-Dinjh, T., and Subirana, J. A. (1996) *Nat. Struct. Biol. 3*, 325−328.
42. Guzikevich-Guerstein, G., and Shakked, Z. (1996) *Nat. Struct. Biol. 3*, 32−37.
43. Cruse, W. B. T., Salisbury, S. A., Brown, T., Cosstick, R., Eckstein, F., and Kennard, O. (1986) *J. Mol. Biol. 192*, 891−905.
44. Kennedy, M. A., Nuutero, S. T., Davis, J. T., Drobny, G. P., and Reid, B. R. (1993) *Biochemistry 32*, 8022−8035.
45. Egli, M., Portmann, S., and Usman, N. (1996) *Biochemistry 35*, 8489−8494.
46. Mujeeb, A., Reynolds, M. A., and James, T. L. (1997) *Biochemistry 36*, 2371−2379.
47. Stec, W. J., Grajkowski, A., Koziolkiewicz, M., and Uznanski, B. (1991) *Nucleic Acids Res. 19*, 5883−5888.
48. Benimetskaya, L., Tonkinson, J. L., Koziolkiewicz, M., Karwowski, B., Guga, P., Zeltser, R., Stec, W., and Stein, C. A. (1995) *Nucleic Acids Res. 23*, 4239−4245.
49. Sierzchala, A., Okruszek, A., and Stec, W. J. (1996) *J. Org. Chem. 61*, 6713−6716.
50. Stec, W. J., Karwowski, B., Bockowska, M., Guga, P., Koziolkiewicz, M., Sochacki, M., Wieczorek, M. W., and Blaszczyk, J. (1998) *J. Am. Chem. Soc. 120*, 7156−7167.

BI9909344